

# A novel UGGT1 and p97-dependent checkpoint for native ectodomains with ionizable intramembrane residue

Jessica Merulla<sup>a,b,c</sup>, Tatiana Soldà<sup>a,b</sup>, and Maurizio Molinari<sup>a,b,d</sup>

<sup>a</sup>Institute for Research in Biomedicine, Protein Folding and Quality Control, CH-6500 Bellinzona, Switzerland;

<sup>b</sup>Università della Svizzera Italiana, CH-6900 Lugano, Switzerland; <sup>c</sup>Graduate School for Cellular and Biomedical

Sciences, University of Bern, CH-3000 Bern, Switzerland; <sup>d</sup>Ecole Polytechnique Fédérale de Lausanne, School of Life Sciences, CH-1015 Lausanne, Switzerland

**ABSTRACT** Only native polypeptides are released from the endoplasmic reticulum (ER) to be transported at the site of activity. Persistently misfolded proteins are retained and eventually selected for ER-associated degradation (ERAD). The paradox of a *structure-based* protein quality control is that *functional* polypeptides may be destroyed if they are architecturally unfit. This has health-threatening implications, as shown by the numerous “loss-of-function” proteopathies, but also offers chances to intervene pharmacologically to promote bypassing of the quality control inspection and export of the mutant, yet functional protein. Here we challenged the ER of human cells with four modular glycopolypeptides designed to alert luminal and membrane protein quality checkpoints. Our analysis reveals the unexpected collaboration of the cytosolic AAA-ATPase p97 and the luminal quality control factor UDP-glucose:glycoprotein glucosyltransferase (UGGT1) in a novel, BiP- and CNX-independent checkpoint. This prevents Golgi transport of a chimera with a native ectodomain that passes the luminal quality control scrutiny but displays an intramembrane defect. Given that human proteopathies may result from impaired transport of functional polypeptides with minor structural defects, identification of quality checkpoints and treatments to bypass them as shown here upon silencing or pharmacologic inhibition of UGGT1 or p97 may have important clinical implications.

## Monitoring Editor

Reid Gilmore

University of Massachusetts

Received: Dec 11, 2014

Revised: Feb 6, 2015

Accepted: Feb 9, 2015

## INTRODUCTION

The protein quality control machineries operating in the mammalian endoplasmic reticulum (ER) lumen examine soluble proteins or the ectodomain of membrane polypeptides in search of nonnative determinants such as hydrophobic patches, unpaired cysteine residues, and nonnative peptidyl-prolyl bonds. Most polypeptides entering the ER are modified with core oligosaccharides (glucose<sub>3</sub>-

mannose<sub>9</sub>-N-acetylglucosamine<sub>2</sub>), which are covalently bound to asparagine side chains (N-linked glycosylation). Their processing is a crucial part of protein quality control. Cycles of deglycosylation/reglycosylation catalyzed by glucosidase II and UDP-glucose:glycoprotein glucosyltransferase (UGGT1) determine retention in the calnexin (CNX) chaperone system and promote formation of native disulfide and peptidyl-prolyl bonds (Caramelo and Parodi, 2008). Complete deglycosylation allows secretion from the ER and transport at the site of activity. Extensive demannosylation catalyzed by members of the glycosyl hydrolase 47 family of  $\alpha$ 1,2-mannosidases (Olivari and Molinari, 2007) triggers selection for dislocation into the cytosol and proteasome-mediated clearance (ER-associated degradation [ERAD]; Brodsky, 2012; Braakman and Hebert, 2013; Merulla et al., 2013).

Structural defects that may prevent polypeptide transport through the secretory pathway include potentially charged (ionizable) residues in the intramembrane domain of membrane-anchored

This article was published online ahead of print in MBoc in Press (<http://www.molbiolcell.org/cgi/doi/10.1091/mbc.E14-12-1615>) on February 18, 2015.

Address correspondence to: Maurizio Molinari ([maurizio.molinari@irb.usi.ch](mailto:maurizio.molinari@irb.usi.ch)).

Abbreviations used:  $\alpha$ 1AT, human  $\alpha$ 1-antitrypsin; CNX, calnexin; DBEQ, N<sup>2</sup>,N<sup>4</sup>-dibenzylquinazoline-2,4-diamine; ER, endoplasmic reticulum; ERAD, ER-associated degradation; NHK, null Hong Kong variant of  $\alpha$ 1AT; TM, transmembrane.

© 2015 Merulla et al. This article is distributed by The American Society for Cell Biology under license from the author(s). Two months after publication it is available to the public under an Attribution–Noncommercial–Share Alike 3.0 Unported Creative Commons License (<http://creativecommons.org/licenses/by-nc-sa/3.0>).

“ASCB®,” “The American Society for Cell Biology®,” and “Molecular Biology of the Cell®” are registered trademarks of The American Society for Cell Biology.

Supplemental Material can be found at:  
<http://www.molbiolcell.org/content/suppl/2015/02/16/mbc.E14-12-1615v1.DC1.html>

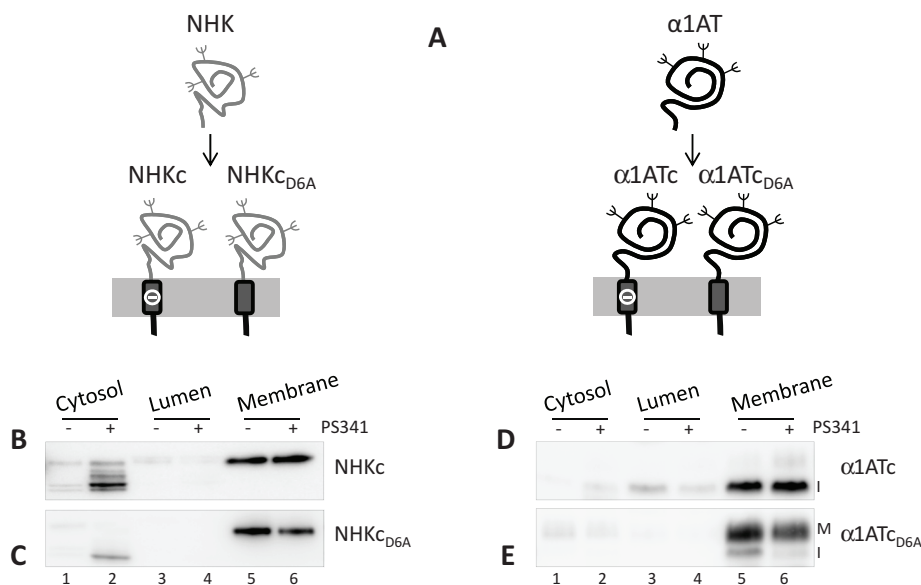


**FIGURE 1:** Chimeras used in this study. (A) The soluble folding-defective NHK or the folding-competent  $\alpha 1$ AT were fused with the transmembrane domain of CD3 $\delta$  carrying an aspartic acid residue (–) in the intramembrane domain to generate the NHKc and  $\alpha 1$ ATc chimeras. The aspartic acid was replaced by an alanine in the NHKc<sub>D6A</sub> and  $\alpha 1$ ATc<sub>D6A</sub> chimeras. (B) Subcellular localization of NHKc in untreated cells (–) or in cells exposed to the proteasome inhibitor PS341 (+). (C) Same as B, for NHKc<sub>D6A</sub>. (D) Same as B, for  $\alpha 1$ ATc (I, immature form of the protein). (E) Same as B for  $\alpha 1$ ATc<sub>D6A</sub> (I, immature; M, mature).

polypeptides (Klausner *et al.*, 1990). Such residues (aspartic and glutamic acids, lysines, and arginines) lower the hydrophobicity of transmembrane (TM) regions (Hessa *et al.*, 2007) and play crucial roles in biogenesis of several oligomeric signaling complexes by insuring retention of orphan subunits to complete complex assembly and degradation of subunits produced in nonstoichiometric amount (Klausner *et al.*, 1990; Call and Wucherpennig, 2005; Feng *et al.*, 2006; Tyler *et al.*, 2012). Mutations that introduce ionizable residues in the intramembrane domain have been linked to loss-of-function diseases such as idiopathic epilepsy (Cossette *et al.*, 2002; Gallagher *et al.*, 2005) or Ehlers–Danlos syndrome (Bin *et al.*, 2014), in which an alanine- or glycine-to-aspartic acid mutation in the TM domain inappropriately tags for degradation functional  $\gamma$ -aminobutyric acid type A (GABA<sub>A</sub>) receptors or ZIP13 proteins, respectively. Idiopathic epilepsy and Ehlers–Danlos syndrome are only two of the hundreds of loss-of-function diseases in which the quality control operating in the secretory pathway, which is based on detection of structural defects, inappropriately prevents transport of functional polypeptides at their final destination. In such cases, the therapeutic interventions that enhance folding, stabilize the mutated polypeptide, or promote bypassing of the transport block are highly sought after (Powers *et al.*, 2009; Guerriero and Brodsky, 2012; Noack *et al.*, 2014).

To understand in more detail the mechanisms regulating protein quality control in the secretory pathway, to understand the consequences of the presence of intramembrane ionizable residues, and to evaluate pharmacologic interventions that promote secretion of inappropriately retained proteins, we monitored the fate of model type I membrane proteins for which a folding-defective (null Hong Kong variant [NHK] of human  $\alpha 1$ -antitrypsin [ $\alpha 1$ AT]) or a folding-competent ectodomain ( $\alpha 1$ AT) were fused to the C-terminal domain of CD3 $\delta$ . This domain contains a naturally occurring integration-competent intramembrane region with an ionizable aspartic acid residue at position 6 (model chimeras NHKc and  $\alpha 1$ ATc), which was replaced by an uncharged alanine residue in the NHKc<sub>D6A</sub> and

$\alpha 1$ ATc<sub>D6A</sub> chimeras (Figure 1A). Our study reveals a novel protein quality checkpoint, which is alerted to prevent secretion of a polypeptide that passes the luminal quality control scrutiny by BiP and CNX but contains an intramembrane ionizable residue. This checkpoint is bypassed upon p97 or UGGT1 silencing or pharmacologic p97 inactivation.

## RESULTS

### The intramembrane ionizable residue does not impair membrane anchoring

To alert and study protein quality checkpoints of the human early secretory pathway, we generated four model chimeric proteins by fusing  $\alpha 1$ AT, a serine protease inhibitor secreted from hepatocytes (Perlmutter, 2011), or NHK, a disease-causing, folding-defective variant thereof (Sifers *et al.*, 1988), with two different membrane anchors. The first anchor corresponds to the TM and cytosolic domains of CD3 $\delta$  and contains a destabilizing ionizable aspartic acid residue at position 6 of the intramembrane region (chimeras  $\alpha 1$ ATc and NHKc), which is replaced by an alanine in the second anchor (chimeras  $\alpha 1$ ATc<sub>D6A</sub> and NHKc<sub>D6A</sub>; Figure

1A). Because ionizable residues in single-pass membrane-anchored proteins increase the free energy of membrane integration ( $\Delta G_{TM}$ ) to levels that may prevent insertion of newly synthesized polypeptides in the lipid bilayer (Shin *et al.*, 1993; Fayadat and Kopito, 2003; Hessa *et al.*, 2007; Feige and Hendershot, 2013), we first controlled membrane association of the four chimeras used in this study. To this end, we performed subcellular fractionation to separate cytosolic (Supplemental Figure S1A, lanes 1 and 2, p97 as marker), luminal (lanes 3 and 4, calreticulin [CRT]), and membrane-associated proteins (lanes 5 and 6, thioredoxin-related transmembrane protein 1 [TMX1]). Efficient membrane integration was confirmed (Figure 1, B–E, lane 5), and only a negligible fraction of the four chimeras was detected in the cytosolic (lane 1) or luminal fractions (lane 3), unless cells were exposed to the proteasome inhibitor PS341 (lanes 2, 4, and 6; see later discussion). This was in good agreement with the calculated  $\Delta G_{TM}$  (<http://dgpred.cbr.su.se>), which predicts efficient membrane integration for the ionizable CD3 $\delta$  TM, which anchors NHKc and  $\alpha 1$ ATc at the membrane ( $\Delta G_{TM} = -0.76$ ), and for the nonionizable CD3 $\delta$  TM, which anchors NHKc<sub>D6A</sub> and  $\alpha 1$ ATc<sub>D6A</sub> ( $\Delta G_{TM} = -2.26$ ).

### An ionizable residue in the TM domain determines higher extractability from the lipid bilayer and faster disposal of a folding-defective ectodomain

NHK is a soluble ERAD substrate, which is dislocated across the ER membrane and degraded by cytosolic proteasomes (Liu *et al.*, 1997). Addition of a membrane anchor with or without an ionizable residue in the TM domain (NHKc and NHKc<sub>D6A</sub>, respectively; Figure 1A) did not change the fate of the folding-defective ectodomain. In fact, both chimeras were efficiently cleared from the ER (Figure 2, A and B, lanes 1–5, and C). To study this, HEK293 cells expressing NHKc or NHKc<sub>D6A</sub> were pulsed with [<sup>35</sup>S]methionine and chased for up to 120 min in the absence of radioactivity. The decay of the immunisolated, radiolabeled chimeras was quantified after their separation in SDS–PAGE (Figure 2, A–C). NHKc had a

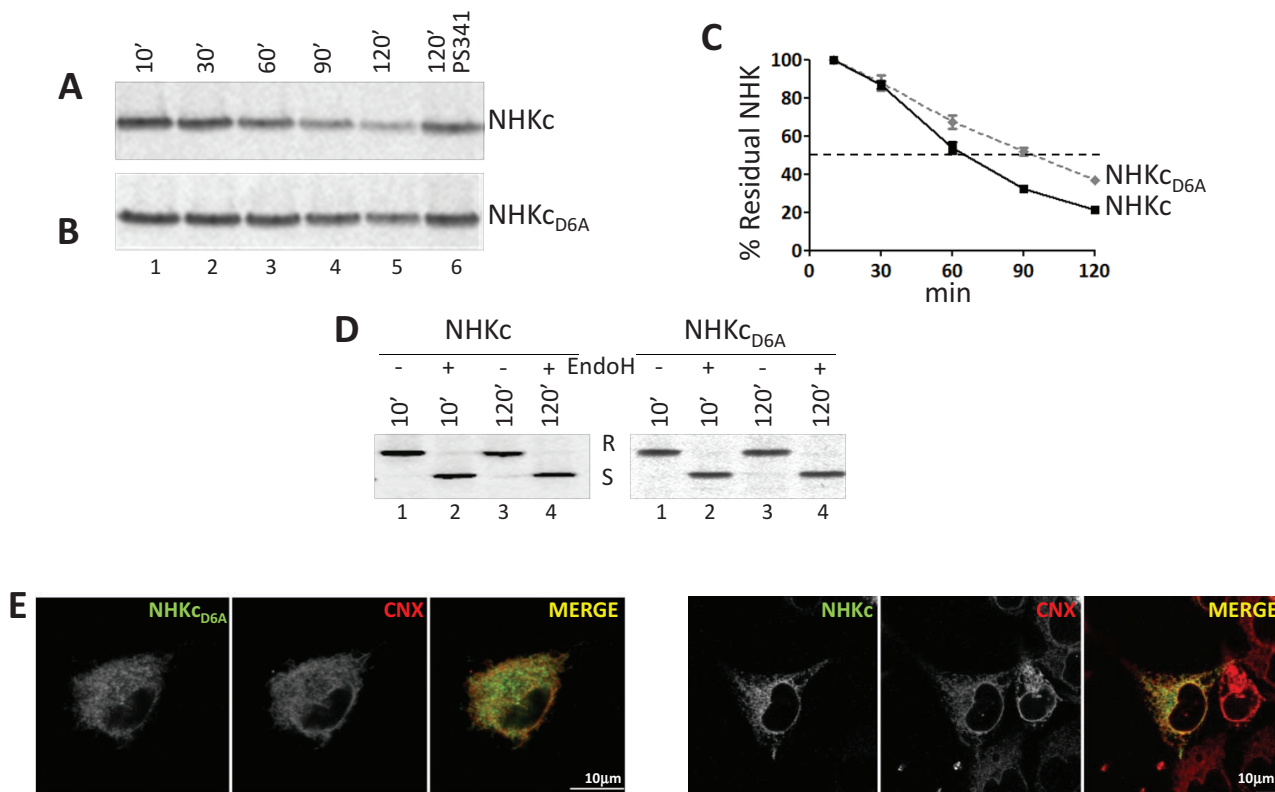


**FIGURE 2:** The ionizable residue in the TM domain accelerates disposal of the folding-defective ectodomain. (A) Stable HEK293 cells expressing NHKc were radiolabeled and chased for up to 120 min without (lanes 1–5) or with the proteasome inhibitor PS341 (lane 6). (B) Same as A, for NHKcD6A. (C) Quantification of NHKc and NHKcD6A decay. Means and SDs are relative to three independent experiments. (D) Normalized amounts of metabolically labeled NHKc and NHKcD6A subjected to EndoH treatment. R, EndoH resistant; S, EndoH sensitive. (E) IF analysis showing colocalization of NHKcD6A and NHKc with the ER marker CNX in HEK293 cells. The chimeras were visualized with an anti-HA tag (left) and CNX with a polyclonal antibody recognizing the endogenous protein (middle). Right, merge. Scale bars, 10  $\mu$ m.

half-life of ~60 min (Figure 2, A, lanes 1–5, and C), which was substantially prolonged by the proteasomal inhibitor PS341, as expected for ERAD substrates (Figure 2A, lane 6). Replacement of the intramembrane ionizable aspartic acid with an alanine delayed the decay of NHKcD6A (half-life of ~90 min; Figure 2, B, lanes 1–5, and C). Consistent with their retention in the ER during preparation for ERAD, both NHKc and NHKcD6A displayed endoglycosidase H (EndoH)–sensitive oligosaccharides (Figure 2D) and colocalized with the ER marker CNX in immunofluorescence (IF; Figure 2E).

Analysis of the subcellular compartmentalization of the misfolded proteins upon inactivation of the proteasomes revealed the substantial accumulation of partially and fully deglycosylated NHKc in the cell cytosol (Figure 1B, lane 2, and Supplemental Figure S1B) to a much larger extent that what was observed for NHKcD6A (Figure 1C, lane 2, and Supplemental Figure S1B). This is consistent with an enhanced extractability from the lipid bilayer of the folding-defective chimera displaying an ionizable residue in the intramembrane space.

### An ionizable residue in the TM domain prevents Golgi transport of the folding-competent $\alpha$ 1AT ectodomain

The foregoing pulse-chase analysis was also used to determine the fate of the chimeras displaying the folding-competent  $\alpha$ 1AT ectodomain tethered at the ER membrane with an anchor containing ( $\alpha$ 1ATc) or not containing ( $\alpha$ 1ATcD6A) the ionizable aspartic acid residue. Analysis of radiolabeled  $\alpha$ 1ATc revealed a major

polypeptide band (I for immature; Figure 3A, lanes 1–5) and a very faint polypeptide with slower electrophoretic mobility appearing at longer chase times (M for mature; Figure 3A, lanes 4 and 5). In the case of  $\alpha$ 1ATcD6A, the fast-migrating polypeptide shown with I was efficiently converted, starting at 30 min of chase, into the slowly migrating M band (Figure 3B, lanes 2–5). Reduction in a glycoprotein's electrophoretic mobility occurs upon release of native proteins from the ER and arrival in the Golgi compartment, where N-linked oligosaccharides are modified to become much larger and resistant to EndoH cleavage (Rothman *et al.*, 1984). An EndoH assay confirmed that  $\alpha$ 1ATc oligosaccharides remained EndoH sensitive throughout the chase (Figure 3, C and E), an indication that this protein was not delivered to the Golgi compartment. In contrast,  $\alpha$ 1ATcD6A oligosaccharides became resistant to EndoH cleavage (Figure 3, D and E), implying that this chimera was efficiently transported to the Golgi. The different intracellular fate of these two chimeras was confirmed in IF. Both proteins colocalized poorly with the ER marker CNX (Figure 3, F and I) and, more significantly, especially  $\alpha$ 1ATcD6A, with intermediate compartment/Golgi markers such as  $\beta$ COP (Figure 3, G and J). In agreement with the biochemical analysis showing that only  $\alpha$ 1ATcD6A displays EndoH-resistant oligosaccharides (Figure 3, D and E), this chimera showed a substantial colocalization with the Golgi marker giantin (Figure 3K), whereas  $\alpha$ 1ATc was virtually excluded from the Golgi (Figure 3H).

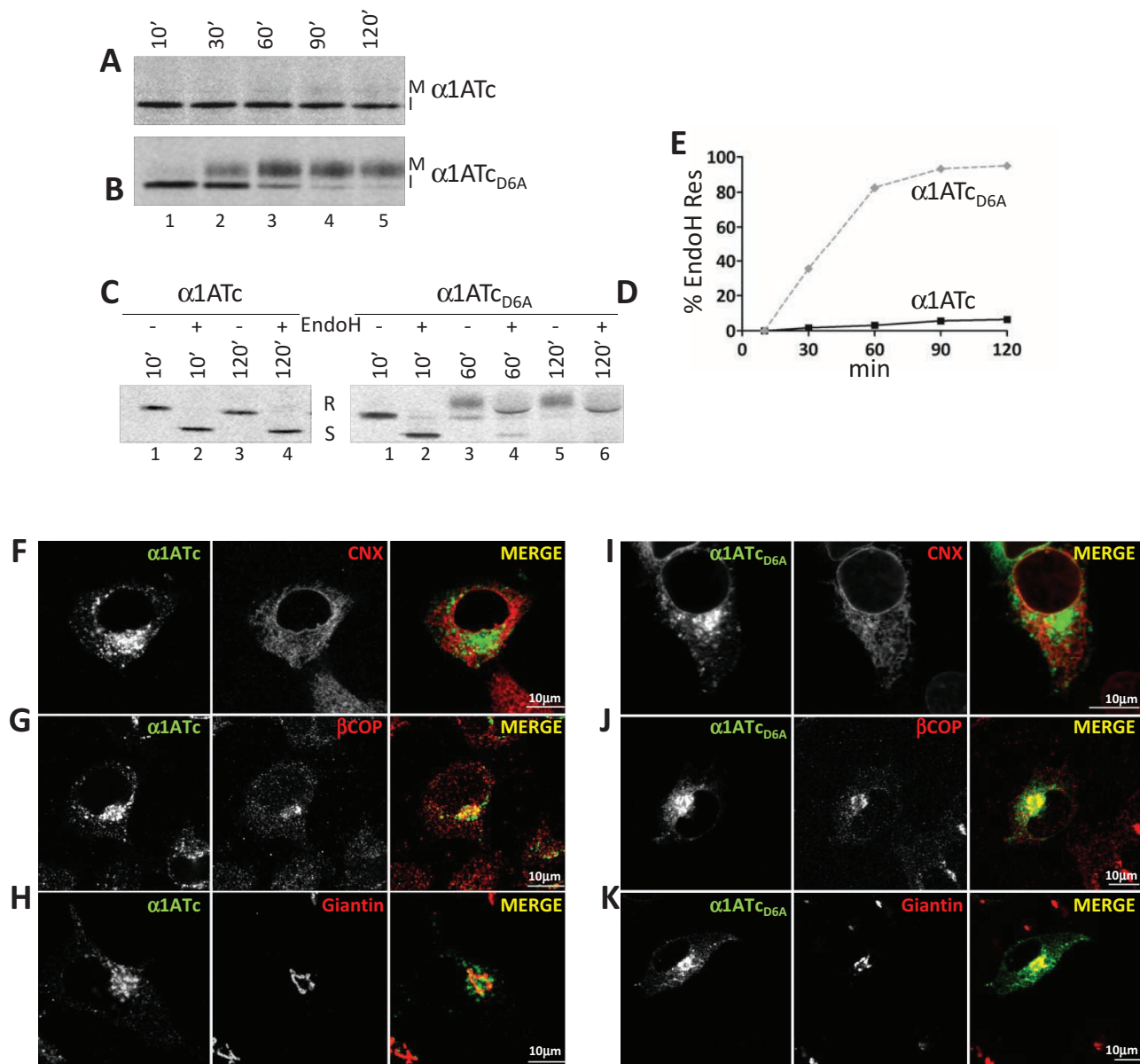


**FIGURE 3:** The ionizable residue in the TM domain retains the native ectodomain in a pre-Golgi compartment. (A) Stable cells expressing  $\alpha 1\text{ATc}$  were radiolabeled and chased for up to 120 min. The fast- and slow-migrating  $\alpha 1\text{ATc}$  are shown (I, immature; M, mature). (B) Same as A, for  $\alpha 1\text{ATc}_{\text{D6A}}$ . (C) Equal amounts of metabolically labeled  $\alpha 1\text{ATc}$  were subjected to EndoH treatment. R, EndoH resistant; S, EndoH sensitive. (D) Same as C, for  $\alpha 1\text{ATc}_{\text{D6A}}$ . (E) Kinetics of acquisition of EndoH-resistant N-glycans. (F) IF analysis showing the colocalization of  $\alpha 1\text{ATc}$  with the ER marker CNX. (G) Same as F, for the ER-Golgi intermediate compartment (ERGIC) marker  $\beta\text{COP}$ . (H) Same as F, for the Golgi marker giantin. (I) Same as F, for  $\alpha 1\text{ATc}_{\text{D6A}}$ . (J) same as G, for  $\alpha 1\text{ATc}_{\text{D6A}}$ . (K) Same as H, for  $\alpha 1\text{ATc}_{\text{D6A}}$ . Scale bars, 10  $\mu\text{m}$ .

### Chimeras with folding-defective ectodomains are persistently reglucosylated and show prolonged association with the ER retention-factors CNX and BiP

Before selection for ERAD, folding-defective polypeptides are retained in the ER upon association with CNX and BiP (Molinari *et al.*, 2002). Here the quality control factor UGT1 plays a crucial role by persistently reglucosylating the oligosaccharides displayed on misfolded conformers, thereby preventing their release from the CNX chaperone system (Caramelo and Parodi, 2008). Persistent protein glucosylation is assessed by a jack bean  $\alpha$ -mannosidase (JB $\alpha$ M) assay. In this assay, JB $\alpha$ M removes eight mannoses from deglycosylated oligosaccharides (Figure 4A, left) but only five from oligosaccharides where branch A is protected by a terminal glucose residue

(Figure 4A, middle). This allows distinction of polypeptides displaying nonglucosylated oligosaccharides, for which the mobility shift upon JB $\alpha$ M treatment is similar to the shift caused by EndoH treatment (Figure 4A, right), from polypeptides displaying glucosylated oligosaccharides, which are characterized by a smaller shift in electrophoretic mobility upon JB $\alpha$ M treatment (Hebert *et al.*, 1995). JB $\alpha$ M treatment performed on NHKc immediately after synthesis (10-min chase, Figure 4B, lanes 1 and 2) or 120 min after synthesis (lanes 3 and 4) caused a smaller shift in electrophoretic mobility than EndoH treatment (lanes 5 and 6). Hence, throughout the chase, NHKc mannoses were protected from complete removal by JB $\alpha$ M. This shows that NHKc is persistently reglucosylated by the glucosylase I or fails to be efficiently deglycosylated by the glucosidase II



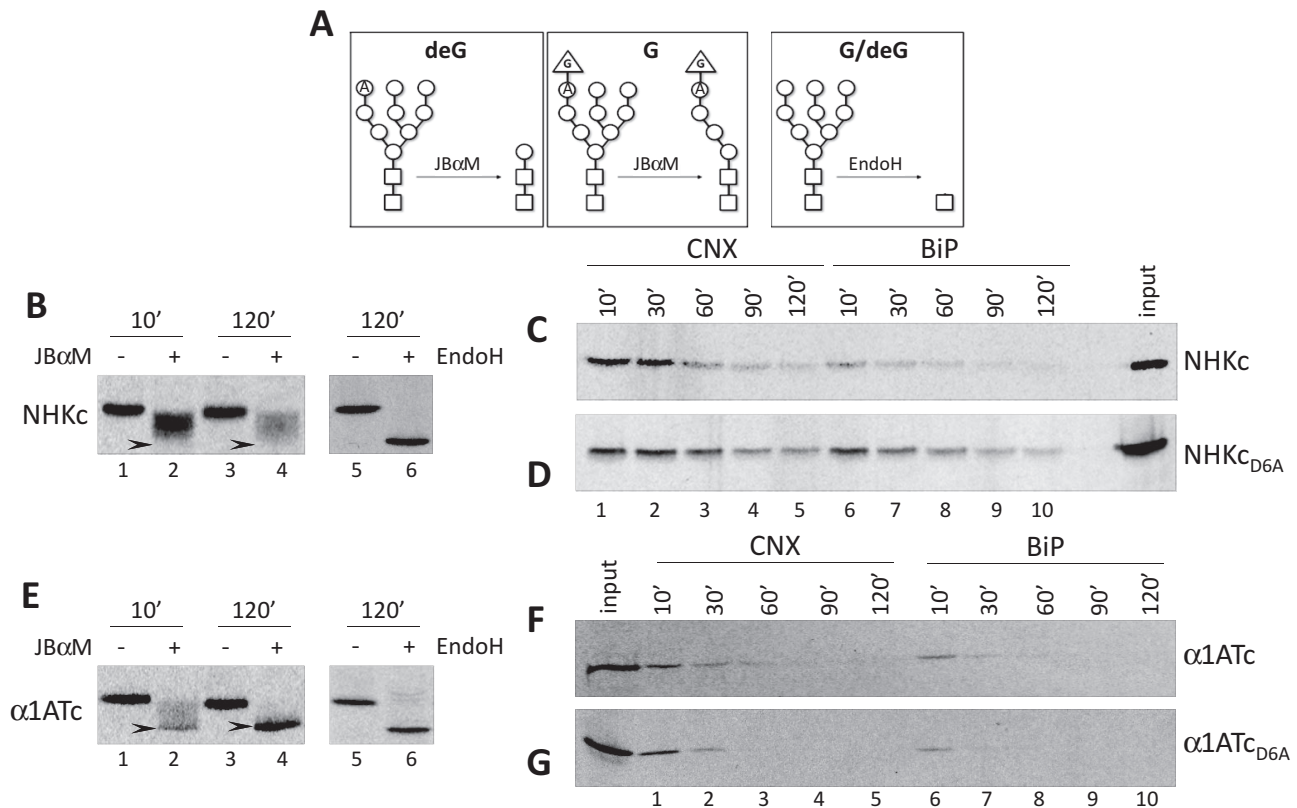


**FIGURE 4:** Glucosylation state and CNX/BiP binding. (A) Schematic representation of the products of JBαM (left and middle) and EndoH activities (right) on nonglucosylated (deG) and glucosylated (G) N-linked glycans. (B) Normalized amount of radiolabeled NHKc at 10- and 120-min chase times were subjected to JBαM (lanes 1–4) or EndoH treatment (lanes 5 and 6). (C) Radiolabeled CNX- (lanes 1–5) and BiP-associated (lanes 6–10) NHKc was immunoprecipitated from stable expressing HEK293 cells. First round of immunoprecipitation with anti-chaperone and second round with anti-chimera antibody. (D) Same as C, for NHKc<sub>D6A</sub>. (E) Same as B, for α1ATc. (F) Same as C, for α1ATc. (G) Same as C, for α1ATc<sub>D6A</sub>.

(arrowheads in Figure 4B, lanes 2 and 4, show where deglucosylated NHKc would run upon JBαM treatment). Consistent with the folding-defective state of their ectodomain, their colocalization with ER markers in IF (Figure 2E), and the persistent reglucosylation (Figure 4B), NHKc and NHKc<sub>D6A</sub> showed a long-lasting association with the ER retention factors CNX (Figure 4, C and D, lanes 1–5) and BiP (lanes 6–10). They did not show detectable association with CRT (Supplemental Figure S2).

The poor colocalization of α1ATc and α1ATc<sub>D6A</sub> with ER chaperones (Figure 3, F–I) shows that their folding-competent ectodomain passes luminal quality control and that the two chimeras are released from the ER. The JBαM assay confirmed the rapid deglucosylation of these chimeras, which allows complete oligosaccharide demannosylation already after a 10-min chase (the case of α1ATc is presented in Figure 4E, lanes 2 and 4). Consistently, both α1ATc and α1ATc<sub>D6A</sub> are rapidly released from CNX and BiP (Figure 4, F and G; they do not associate with CRT; Supplemental Figure S2) and from the ER (Figure 3, F and I). However, only α1ATc<sub>D6A</sub> pursues its transport to the Golgi compartment (Figure 3K), where its oligosaccharides acquire an EndoH-resistant status (Figure 3, B, D, and E). Evidently, the ionizable aspartic acid in the TM domain alerts a quality control device that prevents α1ATc export to the Golgi. This quality control system is clearly unrelated to the *conventional* ER retention-based quality control relying on UGT1, CNX, and BiP, which regulates retention and eventually leads to disposal of the chimeras displaying the folding-defective ectodomain.

### Pharmacologic inactivation of p97 promotes α1ATc transport to the Golgi

To characterize the protein quality checkpoint preventing Golgi transport of α1ATc, we exposed cells for 4 h to low temperature (30°C), chemical chaperones (glycerol), or proteasomal (PS341) or p97 inhibitors (*N*<sup>2</sup>,*N*<sup>4</sup>-dibenzylquinazoline-2,4-diamine [DBEq]), that is, to treatments that bypass retention-based quality control of disease-related polypeptides such as the cystic fibrosis conductance regulator, dystrophin, GABA receptor, ZIP13, and other mutant polypeptides, thereby alleviating disease phenotypes (Denning *et al.*, 1992; Brown *et al.*, 1996; Bonuccelli *et al.*, 2003; Chou *et al.*, 2011; Bin *et al.*, 2014; Han *et al.*, 2015). Only cell treatment with DBeQ substantially enhanced α1ATc secretion to the Golgi, as shown by the appearance of the mature (M in Figure 5, A, lane 6, and B, lane 2 and arrow in lane 5), EndoH-resistant form of α1ATc (Figure 5B, lane 6). IF analysis confirmed that in cells exposed to DBeQ, α1ATc escapes retention-based quality control (Figure 5C) and travels to the Golgi compartment (Figure 5D and quantification). It is worth mentioning that α1ATc retention was not affected by the inactivation of access to the CNX chaperone system with castanospermine (CST; Figure 5A, lane 4), a specific inhibitor of glucosidase I and glucosidase II (Hammond *et al.*, 1994).

To evaluate the selectivity of DBeQ, we compared the fate of NHKc<sub>D6A</sub> and NHKc (subjected to the *conventional* ER quality control), α1ATc<sub>D6A</sub> (efficiently exported to the Golgi), and α1ATc (halted by the DBeQ-sensitive checkpoint) in mock-, PS341-, or

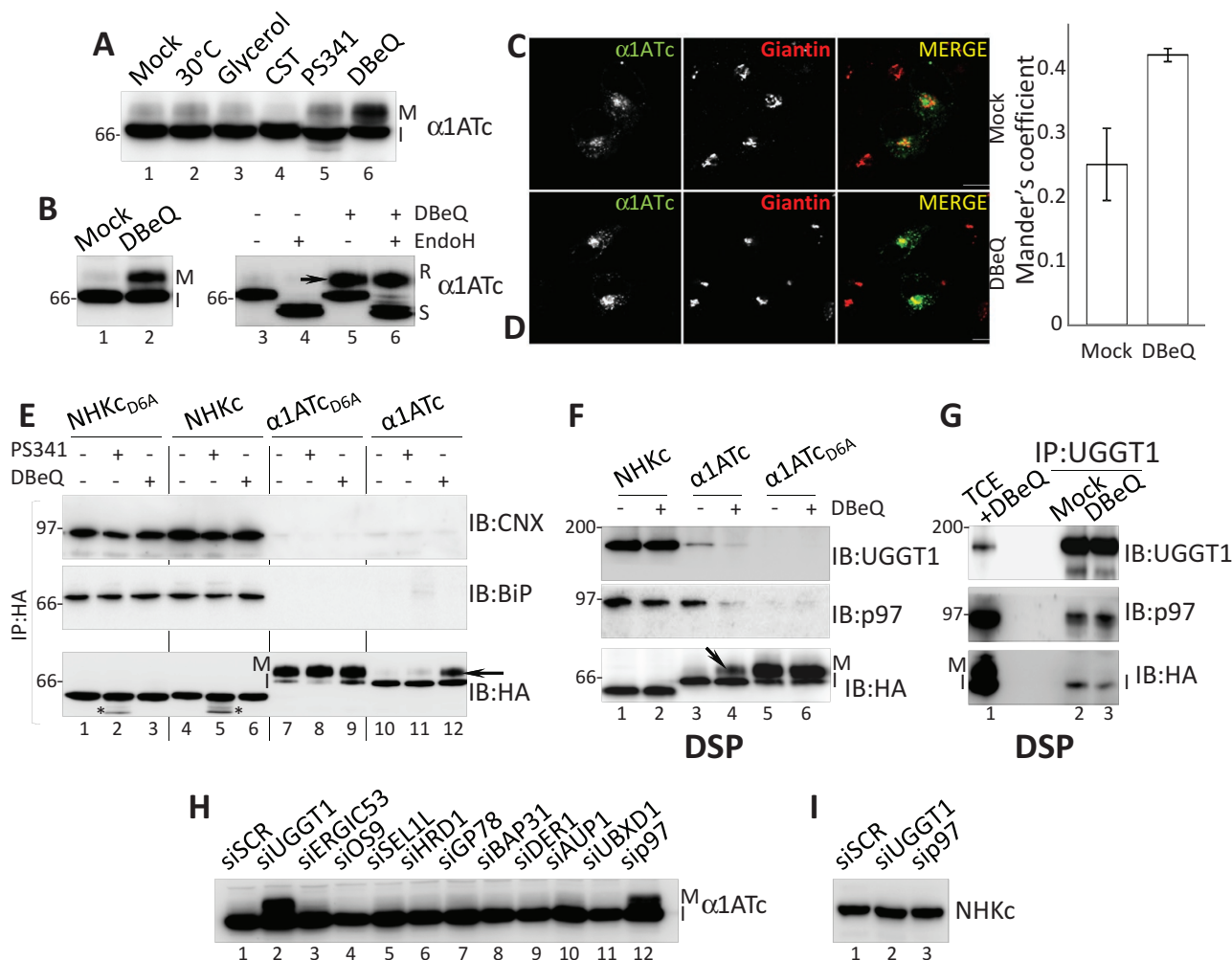


**FIGURE 5:** p97 and UGGT1 participate to the DBE-Q-sensitive protein quality checkpoint. (A)  $\alpha$ 1ATc expressed in cells at 30°C or in cells exposed to glycerol, CST, PS341, or DBE-Q. Only DBE-Q allows production of the mature (M) form of  $\alpha$ 1ATc. (B) The slow-migrating  $\alpha$ 1ATc band is an EndoH-resistant form of the protein (R in lane 6). (C) Same as Figure 3H (lack of  $\alpha$ 1ATc colocalization with the Golgi marker giantin in mock-treated cells). (D) Same as C, in cells treated with DBE-Q.  $\alpha$ 1ATc now colocalizes with giantin. The Manders coefficient shows the colocalization ratio between the green ( $\alpha$ 1ATc) and red channels (giantin) in mock- and DBE-Q-treated cells (Bolte and Cordelières, 2006). (E) Association of NHKcD6A, NHKc,  $\alpha$ 1ATcD6A, and  $\alpha$ 1ATc (used as baits; their amount was normalized) with CNX and BiP in mock-, PS341-, or DBE-Q-treated cells. Bottom, asterisks show deglycosylated NHK chimeras accumulating upon proteasomal inhibition. (F) Same as E, in cells incubated with the chemical cross-linker DSP to stabilize weak associations (NHKc,  $\alpha$ 1ATc, and  $\alpha$ 1ATcD6A were used as bait). (G) Same as F, with UGGT1 as bait. (H) Only silencing of UGGT1 (lane 2) and p97 (lane 12) allows production of mature  $\alpha$ 1ATc. (I) Silencing of UGGT1 and p97 does not affect NHKc retention in the ER.

DBE-Q-treated cells. The chimeras were immunoprecipitated from cell lysates to evaluate changes in the association with the ER-retention factors CNX and BiP (Molinari *et al.*, 2002; Figure 5E, top and middle), as well as variations in their electrophoretic mobility as a straightforward readout for glycoprotein release to the Golgi compartment (Figure 5E, bottom).

The newly synthesized, radiolabeled chimeras with the misfolded ectodomain show persistent association with CNX and BiP (Figure 4, C and D), whereas the chimeras with the native ectodomain are rapidly released from the ER chaperones (Figure 4, F and G). Consistently, at steady state, NHKcD6A and NHKc showed abundant association with the ER-retention factors (Figure 5E, top and middle, lanes 1–6), whereas  $\alpha$ 1ATcD6A and  $\alpha$ 1ATc associated poorly, if at all (lanes 7–12). PS341 and DBE-Q had little effect on the coprecipitation of CNX and BiP with NHKcD6A and NHKc (Figure 5E, top and middle, lane 1 vs. lanes 2 and 3, and lane 4 vs. lanes 5 and 6). The

unchanged electrophoretic mobility of the two chimeras with the folding-defective ectodomain confirmed that DBE-Q did not impair the *conventional* CNX/BiP-mediated quality control that retains them in the ER (Figure 5E, bottom, lane 1 vs. lanes 2 and 3, and lane 4 vs. lanes 5 and 6). DBE-Q did not affect transport to the Golgi of  $\alpha$ 1ATcD6A, as shown by the unchanged attainment of the mature form of this protein (Figure 5E, bottom, lane 7 vs. lane 9), whereas it restored transport to the Golgi of  $\alpha$ 1ATc, as shown by the attainment of the mature polypeptide form (Figure 5, A–D and E, bottom, arrow in lane 12). Thus, pharmacologic inactivation of p97 selectively inactivates the checkpoint alerted by the chimera with the native ectodomain tethered at the membrane with an anchor containing an ionizable residue. Of interest, a similar alanine-to-aspartic acid mutation in the TM domain of the GABA<sub>A</sub> receptor is linked to defective surface transport of the mutant protein causing idiopathic epilepsy (Cossette *et al.*, 2002; Gallagher *et al.*, 2005). The disease

phenotype is alleviated by pharmacologic inactivation or silencing of p97. The recover in mutant GABA<sub>A</sub> receptor secretion has been attributed to the inhibition of the p97 function in ERAD (Han *et al.*, 2015). However, as in the case of  $\alpha$ 1ATc (Figures 5, A, lane 4, and E, lane 11), proteasome inhibition does not restore secretion of the mutant GABA<sub>A</sub> receptor. This leads us to postulate that inhibition of a role of p97 in quality control, rather than in ERAD, may play a role in recovering from loss-of-function diseases as well.

### Pharmacologic inactivation of p97 restores transport to the Golgi of $\alpha$ 1ATc by promoting $\alpha$ 1ATc dissociation from p97 and UGGT1

To confirm the involvement of the DBE<sub>Q</sub> target (i.e., p97) and verify possible involvement in the checkpoint preventing  $\alpha$ 1ATc transport to the Golgi of the quality control factor UGGT1, which cycles in post-ER boundaries (Zuber *et al.*, 2001; Mezzacasa and Helenius, 2002; Gilchrist *et al.*, 2006) and participates in p97-containing complexes (Haines *et al.*, 2012), we analyzed NHKc,  $\alpha$ 1ATc, and  $\alpha$ 1ATC<sub>D6A</sub> associations with p97 and UGGT1 in the presence of the chemical cross-linker dithiobis succinimidyl propionate (DSP) to stabilize weak interactions. This test showed that NHKc and  $\alpha$ 1ATc (Figure 5F, lanes 1–4), but not  $\alpha$ 1ATC<sub>D6A</sub> (lanes 5 and 6), entered complexes with both quality control factors (Figure 5F). Cell incubation with DBE<sub>Q</sub> did not significantly affect the association of p97 and UGGT1 with the ERAD substrate NHKc (lane 1 vs. lane 2), but it substantially decreased the coprecipitation of p97 and UGGT1 with  $\alpha$ 1ATc (lane 3 vs. lane 4). We postulate that in the case of NHK, UGGT1 regulates the reglucosylation that prolongs CNX association, and p97 intervenes in membrane extraction of this ERAD substrate from the ER. In the case of  $\alpha$ 1ATc, which is rapidly released from CNX and is not degraded, the two quality control factors might participate in a novel functional retention complex preventing  $\alpha$ 1ATc secretion. Of note, p97 and UGGT1 have been identified as major interactors of the UBXD1 adaptor protein (Haines *et al.*, 2012) as an indication that they might coexist in functional complexes. Even though we did not detect UBXD1 among the  $\alpha$ 1ATc interactors (unpublished data), the immunoprecipitation of endogenous UGGT1 revealed the coprecipitation of p97 (Figure 5G). DBE<sub>Q</sub> did not disassemble the UGGT1:p97 complex, as shown by the unchanged presence of p97 in immunocomplexes isolated with UGGT1 as bait (Figure 5G, middle, lane 2 vs. lane 3). Instead, the pharmacologic inactivation of p97 caused  $\alpha$ 1ATc release from the two retention factors (Figure 5G, bottom, lane 2 vs. lane 3), thus restoring transport of this chimera to the Golgi.

### p97 and UGGT1 silencing selectively restores transport to the Golgi of $\alpha$ 1ATc

Silencing the expression of a series of early secretory pathway proteins involved in quality control, in ERAD, or in vesicular transport revealed that only p97 and UGGT1 silencing correlated with the complex modification of oligosaccharides, showing transport of  $\alpha$ 1ATc to the Golgi compartment (Figure 5H, lanes 2 and 12, and Supplemental Figure S3). Silencing of p97 and of UGGT1 did not affect the ER retention of the chimeras displaying the misfolded ectodomain (Figure 5I). For p97, this is consistent with the fact that pharmacologic p97 inactivation did not interfere with conventional, retention-based ER quality control (Figure 5E, bottom, lanes 3 and 6, showing the lack of mature NHK<sub>C<sub>D6A</sub></sub> and NHKc forms in cells treated with DBE<sub>Q</sub>).

## DISCUSSION

Human proteopathies may result from inappropriate elimination of functional polypeptides displaying minor structural defects or

delayed attainment of the native structure as a consequence of gene mutations (Lindquist and Kelly, 2011). Thus, the identification and comprehension at the molecular level of the quality checkpoints surveying production of the human proteome is instrumental for designing interventions that counteract their progression. Our data reveal a novel druggable quality checkpoint alerted when the polypeptide's ectodomain fulfills quality control requirements for ER exit but displays other structural defects (in the chimera analyzed in this study, an intramembrane ionizable residue). By showing that cell exposure to DBE<sub>Q</sub> and silencing of p97 restore transport to the Golgi of  $\alpha$ 1ATc, our study identifies p97 as a pharmacologic target to treat loss-of-function proteopathies and underscores the importance of developing function-specific inhibitors of p97 (Chou and Deshaies, 2011).

The cytosolic AAA ATPase p97 is a multifunctional protein (Yamanaka *et al.*, 2012). It participates in a growing number of poorly characterized supramolecular complexes, some of which are involved in ERAD, whereas others contain quality control and vesicular transport factors. The data presented here led us to exclude that transport to the Golgi of  $\alpha$ 1ATc is restored upon inactivation of the function of p97 in ERAD. In fact, proteasome inactivation does not lead to  $\alpha$ 1ATc secretion. Instead, it must be ascribed to a role of p97 in regulating retention of proteins displaying intramembrane defects.

That silencing of p97 would restore  $\alpha$ 1ATc transport to the Golgi was expected because pharmacologic inactivation of p97 does. In contrast, that also UGGT1 silencing would restore  $\alpha$ 1ATc transport was at least partially surprising. In fact,  $\alpha$ 1ATc displays a native ectodomain whose oligosaccharides rapidly lose their terminal glucoses, is rapidly released from CNX, and is therefore most likely not a target of the enzymatic activity of UGGT1. The unperturbed retention of  $\alpha$ 1ATc in cells treated with CST (Figure 5A) confirms that generation of the monoglucosylated form of the  $\alpha$ 1ATc oligosaccharides by the glucosidase I and glucosidase II and/or the persistence of monoglucosylated forms engaging the ER-resident lectin chaperones upon UGGT1 activity is dispensable for the tightness of this novel quality control checkpoint. Nevertheless, UGGT1 cycles in post-ER boundaries (Zuber *et al.*, 2001; Mezzacasa and Helenius, 2002; Gilchrist *et al.*, 2006), might participate in p97-containing supramolecular complexes (Haines *et al.*, 2012), and, as our data imply, participates in DBE<sub>Q</sub>-sensitive complexes that control  $\alpha$ 1ATc retention. Intervention of p97 and of the UGGT1 in the protein quality checkpoint described in this work seems to elude their conventional functions of major components of the ERAD machinery and the CNX cycle, respectively.

The UGGT1/p97 checkpoint complex must contain additional components and, possibly, one or more membrane-spanning proteins that bridge the cytosolic p97 and the luminal UGGT1 (Figure 6). Like p97, the multispanning protein BAP31 is involved in ERAD (Wang *et al.*, 2008) but also in vesicular transport in the early secretory pathway (Bell *et al.*, 2001; Wakana *et al.*, 2008). Significantly, BAP31 shows preferential action on proteins characterized by the presence of ionizable residues in the TM domain (Geiger *et al.*, 2011). As such, BAP31 was a likely candidate to play a role in this novel, DBE<sub>Q</sub>-sensitive protein quality checkpoint that prevents  $\alpha$ 1ATc transport to the Golgi. However, BAP31 silencing did not restore transport to the Golgi of  $\alpha$ 1ATc (Figure 5H, lane 8). This shows that the residual amount (Supplemental Figure S3) of this very abundant protein warrants retention of  $\alpha$ 1ATc or that an elusive, surrogate retention factor can intervene to replace BAP31. Similarly, silencing of several other factors did not reestablish  $\alpha$ 1ATc transport to the Golgi (Figure 5H). Here as well, these factors are not involved in the DBE<sub>Q</sub>-sensitive checkpoint, their silencing was not efficient

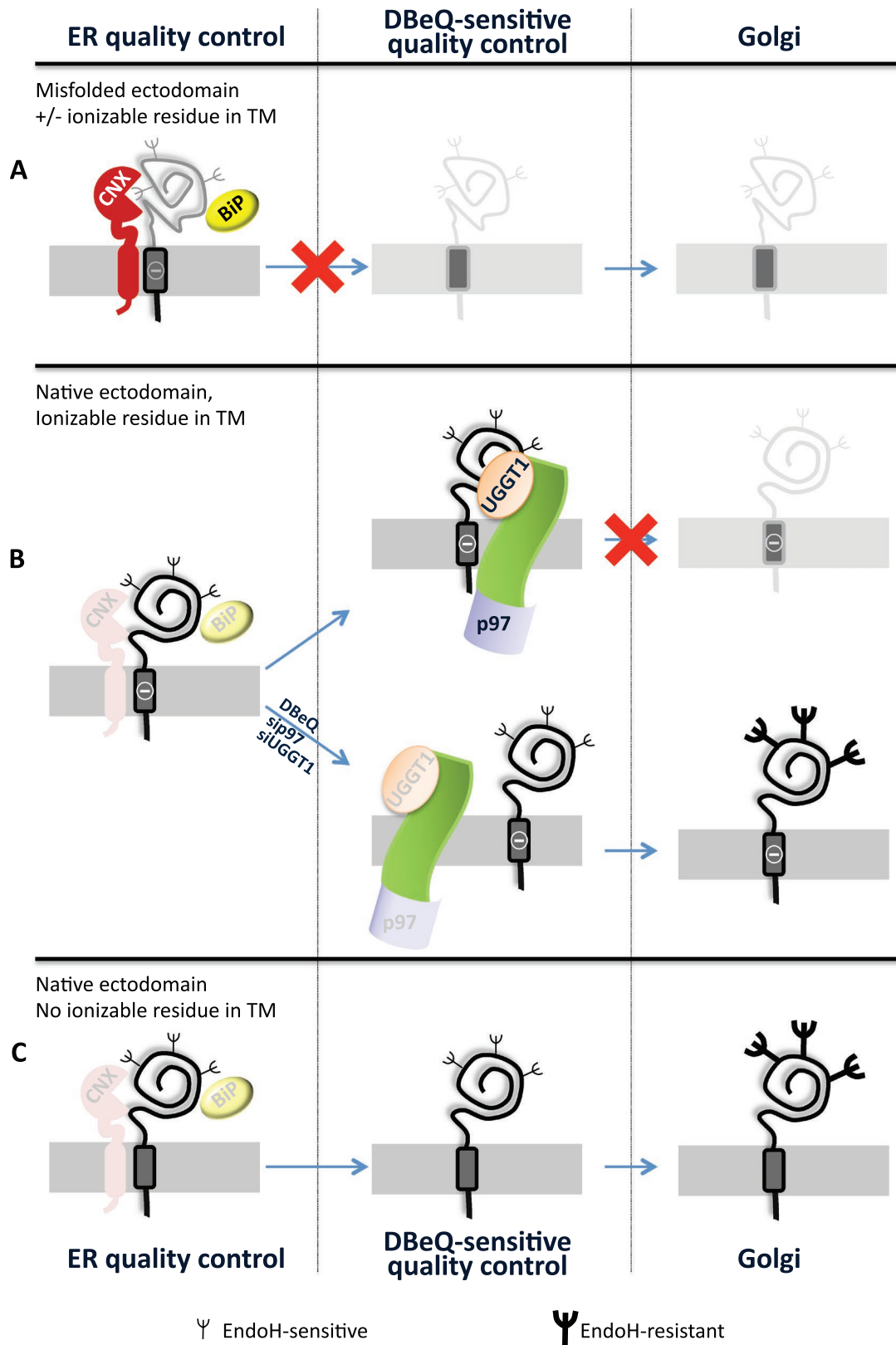


**FIGURE 6:** The chimeras analyzed in this study and their fate. (A) The chimeras with the misfolded ectodomain (NHK<sub>C<sub>D6A</sub></sub> and NHK<sub>C</sub>) are retained in the ER by the *conventional* quality control relying on UGGT1, CNX, and BiP intervention. These proteins are eventually destined to ERAD. (B) The chimera with the native ectodomain, characterized by an ionizable residue in the TM ( $\alpha$ 1AT<sub>C</sub>), fulfills the quality control requirement for release from CNX and BiP, but its transport to the Golgi is halted upon p97 and UGGT1 intervention. This protein quality checkpoint is bypassed upon pharmacologic inhibition of p97 or silencing of p97 or UGGT1 expression. (C) The folding-competent chimera ( $\alpha$ 1AT<sub>C<sub>D6A</sub></sub>) is efficiently transported to the Golgi compartment.



enough to reveal a phenotype, or other factors intervene upon their silencing.

Retention-based quality control is alerted in the early secretory pathway by structural defects that may not compromise the function of the mutant polypeptide yet can prevent the transport of the mutant polypeptide at the site of activity. Secretion of mutant polypeptides linked to cystic fibrosis, muscular dystrophy, idiopathic epilepsy, and lysosomal storage diseases, to name only a few, can be promoted in cultured cells and/or in the organism by chemical or substrate-specific pharmacologic chaperones (Guerriero and Brodsky, 2012; Noack et al., 2014). The development of treatments that alleviate loss-of-function phenotypes caused by hampered trafficking of functional yet structurally defective polypeptides has important medical implications. It relies on the characterization of the mechanisms that regulate quality control and transport at the intracellular or extracellular site of activity of newly synthesized polypeptides. The characterization of a novel, p97-regulated, DBE-Q sensitive quality checkpoint for native ectodomains with intramembrane defects highlights a novel therapeutic avenue to counter the progression of loss-of-function diseases caused by defective transport of functional polypeptides at their final destination.

## MATERIALS AND METHODS

### Expression plasmids, antibodies, and inhibitors

The pCIneo plasmids encoding for CD3 $\delta$  was provided by S. Fang (University of Maryland Biotechnology Institute, Baltimore, MD). The membrane-tethered variants of  $\alpha$ 1ATc ( $\alpha$ 1AT<sub>CD3 $\delta$</sub> ) and NHKc (NHK<sub>CD3 $\delta$</sub> ; Bernasconi et al., 2010) were generated by inserting at the C-terminus of  $\alpha$ 1AT or NHK, both cloned in pcDNA3, residues 97–173 of mouse CD3 $\delta$  (VELDSGTMAGVIFDLIATLLALGVYCFAGHETGRPSGAAEVQALLKNEQLY QPLRDREDTQYSRLGGNWPR-NKKS, transmembrane domain in italic). Commercially available purification kits (Sigma-Aldrich, Buchs, Switzerland) were used for DNA sample preparations. The uncharged versions of  $\alpha$ 1AT<sub>CD6A</sub> and NHK<sub>CD6A</sub> were produced by replacing the aspartic acid residue (D) of the TM sequence (marked in bold) with alanine (A). An Agilent Technologies (Basel, Switzerland) mutagenesis kit was used to prepare the constructs. All proteins were tagged with hemagglutinin (HA) epitope (YPYDVPDYA), and the nucleotide sequences of plasmids were verified on both strands. Antibodies to HA, TMX1, SEL1L, derlin-1 were obtained from Sigma-Aldrich; antibodies to CNX, GP78, HRD1, HERP, derlin-2 and UGGT1 were kind gifts of A. Helenius (ETH, Zurich, Switzerland), S. Fang and R. Wojcikiewicz (SUNY- Upstate Medical University, Syracuse, NY), K. Kokame (Cerebral and Cardiovascular Center, Osaka, Japan), Y. Ye (National Institutes of Health, Bethesda, MD), and A. Parodi (Fundación Instituto Leloir, Buenos Aires, Argentina), respectively. KDEL (BiP-GRP94) was provided by Stressgen (Lausen, Switzerland), BAP31 by Alexis Biochemicals (Lausen, Switzerland),  $\beta$ COP by ABR (Lausen, Switzerland), and ubiquitin by DAKO (Baar, Switzerland). PS-341 (Millennium Pharmaceuticals, Cambridge, MA), DBE-Q, CST, and apyrase (all from Sigma-Aldrich) were used at final concentrations of 10  $\mu$ M, 10  $\mu$ M, 1 mM, and 18 U/ml, respectively.

### Cell lines, transient and stable transfections, and RNA interference

HEK293 cells were grown in DMEM/10% fetal bovine serum (FBS). Transfections were performed with Lipofectamine 2000 (Invitrogen) according to the instructions of the manufacturer. For generation of stable cell lines, cells were selected for 2 wk in DMEM supplemented with 10% FBS and 2% Geneticin. RNA interferences were performed

in HEK293 cells plated at 50–60% confluence on polylysine-coated 3.5-cm Petri dishes. Cells were cotransfected with siRNA duplex (50 pmol/dish; Ambion, Lucerne, Switzerland) and the expression plasmid of interest (0.5  $\mu$ g/dish) using Lipofectamine 2000 (Invitrogen, Lucerne, Switzerland) according to the instructions of the manufacturer. Experiments were performed 48 h after transfection.

### Metabolic labeling, immunoprecipitations, Western blots, and analysis of data

HEK293 cells transiently transfected (18 h after transfection) and stable cell lines were pulsed with 0.05 mCi of [<sup>35</sup>S]methionine/cysteine mix and chased for the indicated time points with DMEM supplemented with 5 mM cold methionine and cysteine. Cell lysates were prepared by solubilization of cells with ice-cold 2% 3-[(3-cholamidopropyl)dimethylammonio]-1-propanesulfonate (CHAPS; or RIPA) in 4-(2-hydroxyethyl)-1-piperazineethanesulfonic acid-buffered saline (HBS) and 20 mM N-ethylmaleimide (NEM) and then centrifuged 10 min at 10,000  $\times$  g. Native immunoprecipitations were performed by adding Protein A beads (Sigma-Aldrich; 1:10 [wt/vol] swollen in HBS) and the selected antibody to cell lysates. Incubations were performed for 2 h at 4°C. The immunoprecipitates were extensively washed (3  $\times$  10 min) with 0.5% CHAPS in HBS or 0.5% Triton X-100, resuspended in sample buffer, incubated at 65°C for 10 min, and separated in SDS-PAGE. To assess chimeras association with CNX and BiP, after immunoisolation of the ER chaperones with the specific antibodies, proteins were denatured with 1% SDS and incubated at 65°C for 10 min, and 1% Triton X-100 was added to the samples. The supernatant obtained after centrifugation (2 min at 10,000  $\times$  g) was used for immunoprecipitation with anti-HA. Relevant bands were quantified by Image Quant software (Molecular Dynamics). Gels were also exposed to BioMax (Kodak) films and scanned with an AGFA scanner. For EndoH (New England Biolabs, Allschwil, Switzerland) treatment, immunisolated chimeras were incubated for 2 h at 37°C. Samples were then analyzed in reducing SDS-PAGE. Western blots were performed with blocking polyvinylidene difluoride (PVDF) membranes with 10% (wt/vol) milk (Bio-Rad, Cressier, Switzerland) and using primary antibodies at 1:1000 to 1:3000 dilution. Secondary antibodies were horseradish peroxidase conjugated and used at 1:20,000 to 1:40,000 dilution. The Luminata Forte ECL detection system was from Millipore (Schaffhausen, Switzerland), and signal was detected using ImageQuant LAS 4000 (GE Healthcare, Glattbrugg, Switzerland).

### Jack bean $\alpha$ -mannosidase assay

Protein glucosylation state was monitored by JB $\alpha$ M assay as described in Hebert et al. (1995).

### Carbonate extraction

For carbonate extraction, cells were seeded in 6-cm dishes (polylysine-coated) and washed in PBS and PBS-NEM. Cells were then resuspended in 10 mM triethanolamine, 10 mM acetic acid, 250 mM sucrose, 1 mM EDTA, pH 7.4, and 20 mM NEM and were broken by four to six passages through a 1-ml, 25-gauge needle syringe. Nuclei were removed by 2  $\times$  1000  $\times$  g centrifugation. The supernatant was centrifuged at 200,000  $\times$  g in TLA-120.2 rotor for 45 min. The supernatant obtained (cytosol) was recovered, and the pellet fraction was resuspended in 500  $\mu$ l of 100 mM Na<sub>2</sub>CO<sub>3</sub> and incubated for 25 min on ice. Samples were then centrifuged for 45 min at 200,000  $\times$  g. The supernatant (lumen) was harvested and the pellet was rinsed with 500  $\mu$ l of 100 mM Na<sub>2</sub>CO<sub>3</sub> and subjected to further centrifugation at 200,000  $\times$  g for 35 min. The pellet was solubilized in RIPA on ice (20 min), and the membrane-bound

fraction was rescued after further centrifugation for 10 min at 200,000 × g. Normalized quantities of fractions were loaded on SDS–PAGE and transferred on PVDF membranes, and immunoblot was performed as previously described.

### Indirect immunofluorescence microscopy

Stable HEK293 cells were plated 17 h before fixation on polylysine-coated coverslips. Cells were washed twice with PBS and fixed at room temperature for 20 min with 3.7% formaldehyde diluted in PBS. Cells were washed (3× 5 min) with PBS and incubated in permeabilization solution (0.1% Triton X-100 in PBS) for 15 min to improve antigen accessibility. Washings in PBS (3× 5 min) were performed before 30-min incubation with 10% FBS diluted in PBS (blocking solution). Cells were incubated for at least 1 h, 30 min with primary antibodies diluted 1:50 to 1:100 in blocking solution, washed three times (PBS), and incubated with Alexa Fluor–conjugated secondary antibodies (Invitrogen) diluted 1:200 in blocking solution for at least 45 min. Cells were rinsed with PBS (three for 5 min each) and H<sub>2</sub>O and mounted with Vectashield (Vector Laboratories) supplemented with 4',6-diamidino-2-phenylindole. Images were collected using a laser scanning confocal microscope (Leica DL6000 microscope stand connected to a SP5 scan head). ImageJ software (National Institutes of Health, Bethesda, MD) was used for image analysis and processing.

### Cross-linking assay

HEK293 cells were seeded in 3.5-cm polylysine-coated dishes 17 h before treatment. Immediately before use, DSP (Sigma-Aldrich) was prepared at 100× final concentration in dimethyl sulfoxide. Cells were washed once with PBS and incubated for 30 min at room temperature in PBS supplemented with 1 mM DSP. The reaction was quenched by incubating cells with PBS and 20 mM Tris, pH 7.8, for 15 min.

### ACKNOWLEDGMENTS

We thank F. Fumagalli for technical help; S. Fang, H. Farhan, R. Geiger, A. Helenius, H. Ploegh, A. Parodi, Z. Ronai, K. Kokame, Y. Ye, and R. Wojcikiewicz for various reagents; and members of M.M.'s lab for critical reading of the manuscript. M.M. is supported by Signora Alessandra, the Foundation for Research on Neurodegenerative Diseases, the Swiss National Science Foundation, and the Comel, Gabriele, and Gelu Foundations.

### REFERENCES

Bell AW, Ward MA, Blackstock WP, Freeman HN, Choudhary JS, Lewis AP, Chotai D, Fazel A, Gushue JN, Paiement J, et al. (2001). Proteomics characterization of abundant Golgi membrane proteins. *J Biol Chem* 276, 5152–5165.

Bernasconi R, Galli C, Calanca V, Nakajima T, Molinari M (2010). Stringent requirement for HRD1, SEL1L, and OS-9/XTP3-B for disposal of ERAD-L substrates. *J Cell Biol* 188, 223–235.

Bin BH, Hojyo S, Hosaka T, Bhin J, Kano H, Miyai T, Ikeda M, Kimura-Someya T, Shirouzu M, Cho EG, et al. (2014). Molecular pathogenesis of spondylocheirodysplastic Ehlers-Danlos syndrome caused by mutant ZIP13 proteins. *EMBO Mol Med* 6, 1028–1042.

Bolte S, Cordelieres FP (2006). A guided tour into subcellular colocalization analysis in light microscopy. *J Microsc* 224, 213–232.

Bonuccelli G, Sotgia F, Schubert W, Park DS, Frank PG, Woodman SE, Insabato L, Cammer M, Minetti C, Lisanti MP (2003). Proteasome inhibitor (MG-132) treatment of mdx mice rescues the expression and membrane localization of dystrophin and dystrophin-associated proteins. *Am J Pathol* 163, 1663–1675.

Braakman I, Hebert DN (2013). Protein folding in the endoplasmic reticulum. *Cold Spring Harb Perspect Biol* 5, a013201.

Brodsky JL (2012). Cleaning up: ER-associated degradation to the rescue. *Cell* 151, 1163–1167.

Brown CR, Hong-Brown LQ, Biwersi J, Verkman AS, Welch WJ (1996). Chemical chaperones correct the mutant phenotype of the delta F508 cystic fibrosis transmembrane conductance regulator protein. *Cell Stress Chaperones* 1, 117–125.

Call ME, Wucherpennig KW (2005). The T cell receptor: critical role of the membrane environment in receptor assembly and function. *Annu Rev Immunol* 23, 101–125.

Caramelo JJ, Parodi AJ (2008). Getting in and out from calnexin/calreticulin cycles. *J Biol Chem* 283, 10221–10225.

Chou TF, Brown SJ, Minond D, Nordin BE, Li K, Jones AC, Chase P, Porubsky PR, Stoltz BM, Schoenen FJ, et al. (2011). Reversible inhibitor of p97, DBeQ, impairs both ubiquitin-dependent and autophagic protein clearance pathways. *Proc Natl Acad Sci USA* 108, 4834–4839.

Chou TF, Deshaies RJ (2011). Development of p97 AAA ATPase inhibitors. *Autophagy* 7, 1091–1092.

Cossette P, Liu L, Brisebois K, Dong H, Lortie A, Vanasse M, Saint-Hilaire JM, Carman L, Verner A, Lu WY, et al. (2002). Mutation of GABRA1 in an autosomal dominant form of juvenile myoclonic epilepsy. *Nat Genet* 31, 184–189.

Denning GM, Anderson MP, Amara JF, Marshall J, Smith AE, Welsh MJ (1992). Processing of mutant cystic fibrosis transmembrane conductance regulator is temperature-sensitive. *Nature* 358, 761–764.

Fayadat L, Kopito RR (2003). Recognition of a single transmembrane degon by sequential quality control checkpoints. *Mol Biol Cell* 14, 1268–1278.

Feige MJ, Hendershot LM (2013). Quality control of integral membrane proteins by assembly-dependent membrane integration. *Mol Cell* 51, 297–309.

Feng J, Call ME, Wucherpennig KW (2006). The assembly of diverse immune receptors is focused on a polar membrane-embedded interaction site. *PLoS Biol* 4, e142.

Gallagher MJ, Shen W, Song L, Macdonald RL (2005). Endoplasmic reticulum retention and associated degradation of a GABAA receptor epilepsy mutation that inserts an aspartate in the M3 transmembrane segment of the alpha1 subunit. *J Biol Chem* 280, 37995–38004.

Geiger R, Andrichke D, Friebe S, Herzog F, Luisoni S, Heger T, Helenius A (2011). BAP31 and BiP are essential for dislocation of SV40 from the endoplasmic reticulum to the cytosol. *Nat Cell Biol* 13, 1305–1314.

Gilchrist A, Au CE, Hiding J, Bell AW, Fernandez-Rodriguez J, Lesimple S, Nagaya H, Roy L, Gosline SJ, Hallett M, et al. (2006). Quantitative proteomics analysis of the secretory pathway. *Cell* 127, 1265–1281.

Guerriero CJ, Brodsky JL (2012). The delicate balance between secreted protein folding and endoplasmic reticulum-associated degradation in human physiology. *Physiol Rev* 92, 537–576.

Haines DS, Lee JE, Beauparlant SL, Kyle DB, den Besten W, Sweredoski MJ, Graham RL, Hess S, Deshaies RJ (2012). Protein interaction profiling of the p97 adaptor UBXD1 points to a role for the complex in modulating ERGIC-53 trafficking. *Mol Cell Proteomics* 11, M111.016444.

Hammond C, Braakman I, Helenius A (1994). Role of N-linked oligosaccharide recognition, glucose trimming, and calnexin in glycoprotein folding and quality control. *Proc Natl Acad Sci USA* 91, 913–917.

Han DY, Di XJ, Fu YL, Mu TW (2015). Combining valosin-containing protein (VCP) inhibition and suberanilohydroxamic acid (SAHA) treatment additively enhances the folding, trafficking, and function of epilepsy-associated gamma-aminobutyric acid, type A (GABAA) receptors. *J Biol Chem* 290, 325–337.

Hebert DN, Foellmer B, Helenius A (1995). Glucose trimming and glucosylation determine glycoprotein association with calnexin in the endoplasmic reticulum. *Cell* 81, 425–433.

Hessa T, Meindl-Beinker NM, Bernsel A, Kim H, Sato Y, Lerch-Bader M, Nilsson I, White SH, von Heijne G (2007). Molecular code for transmembrane-helix recognition by the SecE1 translocon. *Nature* 450, 1026–1030.

Klausner RD, Lippincott-Schwartz J, Bonifacio JS (1990). The T cell antigen receptor: insights into organelle biology. *Annu Rev Cell Biol* 6, 403–431.

Lindquist SL, Kelly JW (2011). Chemical and biological approaches for adapting proteostasis to ameliorate protein misfolding and aggregation diseases: progress and prognosis. *Cold Spring Harb Perspect Biol* 3, a004507.

Liu Y, Choudhury P, Cabral CM, Sifers RN (1997). Intracellular disposal of incompletely folded human alpha1-antitrypsin involves release from

- calnexin and post-translational trimming of asparagine-linked oligosaccharides. *J Biol Chem* 272, 7946–7951.
- Merulla J, Fasana E, Solda T, Molinari M (2013). Specificity and regulation of the endoplasmic reticulum-associated degradation machinery. *Traffic* 14, 767–777.
- Mezzacasa A, Helenius A (2002). The transitional ER defines a boundary for quality control in the secretion of tsO45 VSV glycoprotein. *Traffic* 3, 833–849.
- Molinari M, Galli C, Piccaluga V, Pieren M, Paganetti P (2002). Sequential assistance of molecular chaperones and transient formation of covalent complexes during protein degradation from the ER. *J Cell Biol* 158, 247–257.
- Noack J, Brambilla Pisoni G, Molinari M (2014). Proteostasis: bad news and good news from the endoplasmic reticulum. *Swiss Med Wkly* 144, w14001.
- Olivari S, Molinari M (2007). Glycoprotein folding and the role of EDEM1, EDEM2 and EDEM3 in degradation of folding-defective glycoproteins. *FEBS Lett* 581, 3658–3664.
- Perlmutter DH (2011). Alpha-1-antitrypsin deficiency: importance of proteasomal and autophagic degradative pathways in disposal of liver disease-associated protein aggregates. *Annu Rev Med* 62, 333–345.
- Powers ET, Morimoto RI, Dillin A, Kelly JW, Balch WE (2009). Biological and chemical approaches to diseases of proteostasis deficiency. *Annu Rev Biochem* 78, 959–991.
- Rothman JE, Urbani LJ, Brands R (1984). Transport of protein between cytoplasmic membranes of fused cells: correspondence to processes reconstituted in a cell-free system. *J Cell Biol* 99, 248–259.
- Shin J, Lee S, Strominger JL (1993). Translocation of TCR alpha chains into the lumen of the endoplasmic reticulum and their degradation. *Science* 259, 1901–1904.
- Sifers RN, Brashears-Macatee S, Kidd VJ, Muensch H, Woo SL (1988). A frameshift mutation results in a truncated alpha 1-antitrypsin that is retained within the rough endoplasmic reticulum. *J Biol Chem* 263, 7330–7335.
- Tyler RE, Pearce MM, Shaler TA, Olzmann JA, Greenblatt EJ, Kopito RR (2012). Unassembled CD147 is an endogenous ER-associated degradation (ERAD) substrate. *Mol Biol Cell* 23, 4668–4678.
- Wakana Y, Takai S, Nakajima K, Tani K, Yamamoto A, Watson P, Stephens DJ, Hauri HP, Tagaya M (2008). Bap31 is an itinerant protein that moves between the peripheral endoplasmic reticulum (ER) and a juxtanuclear compartment related to ER-associated Degradation. *Mol Biol Cell* 19, 1825–1836.
- Wang B, Heath-Engel H, Zhang D, Nguyen N, Thomas DY, Hanrahan JW, Shore GC (2008). BAP31 interacts with Sec61 translocons and promotes retrotranslocation of CFTRDeltaF508 via the derlin-1 complex. *Cell* 133, 1080–1092.
- Yamanaka K, Sasagawa Y, Ogura T (2012). Recent advances in p97/VCP/Cdc48 cellular functions. *Biochim Biophys Acta* 1823, 130–137.
- Zuber C, Fan JY, Guhl B, Parodi A, Fessler JH, Parker C, Roth J (2001). Immunolocalization of UDP-glucose:glycoprotein glucosyltransferase indicates involvement of pre-Golgi intermediates in protein quality control. *Proc Natl Acad Sci USA* 98, 10710–10715.